PAPER • OPEN ACCESS

Validation of the real-time-response ProCap measurement system for full field wake scans behind a yawed model-scale wind turbine

View the article online for updates and enhancements.

IOP ebooks™

Bringing you innovative digital publishing with leading voices to create your essential collection of books in STEM research.

Start exploring the collection - download the first chapter of every title for free.

Validation of the real-time-response ProCap measurement system for full field wake scans behind a yawed model-scale wind turbine

Jan Bartl[1], Andreas Müller[2], Andrin Landolt[3], Franz Mühle[4], Mari Vatn[1], Luca Oggiano[1,5], Lars Sætran[1]

[1] Norges teknisk-naturvitenskapelige universitet (NTNU), Trondheim, Norway
[2] ETH Zürich, Zürich, Switzerland
[3] streamwise gmbh, Männedorf, Switzerland
[4] Norges miljø- og biovitenskapelige universitet (NMBU), Ås, Norway
[5] Institutt for Energiteknikk (IFE), Kjeller, Norway

E-mail: `jan.bartl@ntnu.no, landolt@streamwise.ch`

Abstract. For an accurate prediction of the complex flow conditions in wind farms, model scale wake flow measurements represent important references in well-defined boundary conditions. State-of-the art flow measurement techniques are often time-expensive and require elaborate post-processing to assess the data quality. In this wind tunnel study we demonstrate the advantages of the real-time-response system Probe Capture (ProCap) for measurements of a complex three-dimensional wind turbine wake flow. The complex wake flow behind a yawed model wind turbine is measured with both a Laser-Doppler Anemometer (LDA) and the ProCap system. Both the streamwise and vertical flow component show an accurate agreement with the LDA reference experiment for various measured downstream distances and turbine yaw angles. Areas of strong rotation in the wake flow are accurately resolved by the ProCap measurement system confirming its applicability for wind turbine wake measurement. The system appears to greatly facilitate and speed up larger wake surveys by a factor of 30 and thus has the potential to enhance the understanding of the complex flow topology in wind turbine wakes.

1. Introduction

The complex wake flow behind a yawed wind turbine has become a widely discussed topic in wind farm optimization research. As single wind turbines are often exposed to the low-kinetic-energy flow of an upstream turbine, wake redirection through intentional yaw misalignment can possibly offer benefits for the combined wind farm power output [1]. A couple of wind tunnel experiments on the wake flow behind a yawed turbine have recently been conducted showing a clearly deflected [2] and also curled wake shape [3, 4]. Large-eddy-simulations (LES) by Vollmer et al. [5] furthermore showed a strong dependency of the yawed wake's shape and deflection on the atmospheric stability. This dependency was further investigated by Bartl et al. [6], who performed a wind tunnel experiment on the wake of a yawed wind turbine exposed to different turbulent inflow conditions. The study concluded on a significant influence of the turbulence level on the wake's shape and deflection. The same experimental setup was used in a study by Schottler et al. [7], who showed a ring of increased intermittency around the mean velocity

deficit area on a yawed wake, suggesting a significantly wider area of wake impact than estimated hitherto. The same experimental results have furthermore been used for a blind test comparison of numerical simulation models. Mühle et al. [8] compared the yawed wake flow behind one and two rotors with four different high-fidelity numerical predictions, confirming the mature development stage of LES and Detached-eddy-simulations (DES) for wind turbine wake simulations.

The computational fluid dynamics (CFD) models have to be validated with well-defined reference experiments. For some turbine operating states, for instance yawed rotors, the wake flow becomes highly complex and three-dimensional. Therefore, measurements over a two- or three dimensional grid of measurement points have to be performed in order to capture the complex characteristics. Due to the required spatial resolution, these types of measurements are very time consuming and the results become only available by post-processing the data at the end of the measurements. A much faster recording process, which delivers accurate data in real-time is therefore desirable.

2. Objectives
The objective of this study is two-fold. The primary objective is to validate the ProCap (Probe Capture) system, an innovative approach for flow measurements, for the complex flow of a model scale wind turbine wake. The time-averaged flow components measured by the ProCap measurement system are therefore compared to reference data of a two component Laser-Doppler Anemometer (LDA) system. The high spatial resolution and accuracy of ProCap and its short setup and measurement time are demonstrated and discussed.

As a secondary objective the wake flow behind a yawed wind turbine model is analyzed in dependency of the turbine yaw angle and the downstream distance up to x/D=15. Aside from an study of the wake three-dimensional shape, a comparison of the far wake deflection with analytical wake models by Jiménez et al. [9] and Bastankhah and Porte-Agél [4] is performed.

3. Methods
3.1. Wind tunnel and turbine models
The experiments were performed in the slow speed wind tunnel at the Department of Energy and Process Engineering at the Norwegian University of Science and Technology. The wind tunnel has a cross section of $(z \times y) = 2.7\,m \times 1.8\,m$ and a total length of $x = 11.0\,m$. The inlet velocity is kept constant at $u_{ref} = 10.0\,m/s$ throughout the entire experiment, at which the clean inflow features a low turbulence intensity of $TI = 0.23\%$. The model wind turbine has a rotor diameter of $D = 0.45\,m$, which is a downscaled version of the rotor previously used in wind tunnel experiments at NTNU [2, 6, 8]. The downscaled rotor blocks less than 3% of the wind tunnel cross-sectional area, which supports the assumption that sidewall blockage on the deflected wake flow can be neglected. However, the Reynolds number on the blade tips s in the range of $Re_{tip} = 50 \times 10^4$. In this range, the rotor's NREL S826 airfoil is operated in a highly transitional flow regime as shown by Sarmast and Mikkelsen [10]. Yet, the effects of this complex blade flow on the far wake of a wind turbine are deemed to be negligible [11]. The turbine is installed $x = 2.71\,m$ from the tunnel inlet, while the hub height is adjusted to $y_{hub} = 0.90\,m$ which corresponds to the center of the wind tunnel. The turbine is operated at it optimum tip speed ratio at $\lambda = 3.5$. At a yaw angle of $\gamma = 0°$, the turbine reaches a maximum power coefficient of $C_{P,0°} = 0.35$ and thrust coefficient of $C_{T,0°} = 0.73$. When the turbine is yawed to $\gamma = 30°$, both power and thrust are reduced. A power coefficient of $C_{P,30°} = 0.21$ and thrust coefficient of $C_{T,30°} = 0.63$ are measured. More details of the turbine's operating characteristics are documented in Garcia et al. [12].
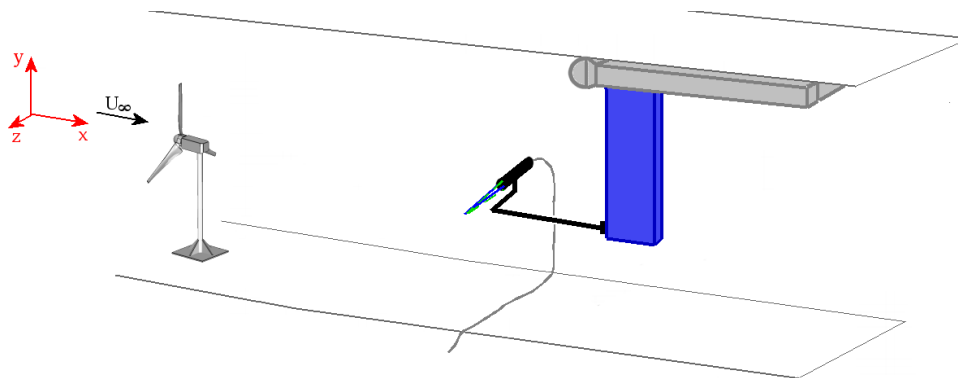
Figure 1. A two-component LDA probe installed on a traversing system in the wind tunnel is applied for reference wake measurements downstream of the model wind turbine. The wind tunnel side walls (not shown in sketch) are located at $z/R = \pm 6$, while the floor and roof are located at $y/R = \pm 4$.

3.2. Laser-Doppler anemometry (LDA)

For the present study two different flow measurement techniques are applied to measure the wake flow behind a wind turbine. As a reference, the well-established technique Laser-Doppler anemometry is used. A sketch of the LDA system installed on the traversing system in the wind tunnel is shown in Figure 1. The traversing system is located underneath the roof inside the wind tunnel, blocking about 10% of the wind tunnel cross sectional area. The traversing system thus influences the streamwise and vertical flow in locations close to where the blockage occurs. The anemometer is a two-component Dantec FiberFlow system, which is applied in Differential Doppler Mode. The sampling rate of the LDA is not constant, as the Doppler-shift-frequency of the scattering by a randomly passing particle is measured. For this purpose, a flow smoke is injected into the wind tunnel at constant time intervals. The smoke particles are assumed to be evenly distributed in the flow and have a size between 0.5-20 μm. The two component Laser probe is mounted on a traversing system in the wind tunnel, which is manually operated from the control computer. An automated scanning of a defined grid of measurement points would be possible, but due to reoccurring manual cleaning of the laser lens not feasible. In order to keep the total measurement time under 5 hours, a spatial resolution of 4.5 cm is chosen, corresponding to 357 measurement point per full wake scan. For every measurement points 5×10^4 samples are recorded over a period of approximately $30s$, resulting in an average sampling frequency of $1666 Hz$. The measurement grid of the LDA scans is shown in Figure 3. The data of the two recorded velocity components is stored in tables and has to be post-processed in order to obtain a visual of the flow.

3.3. Probe Capture anemometry (ProCap)

The ProCap system consists of a hand-guided 5-hole pressure probe, whose instantaneous position is tracked in real time by a motion capture camera system. A sketch of the ProCap system set up in the wind tunnel is shown in Figure 2. The probe's position an alignment is tracked on a sub-millimeter scale by the infrared cameras through reflective passive markers on the probe. The tracking rate of $200 Hz$ ensures that each measurement point can be attributed to a position in the volume of interest. A sketch of the camera system and the hand-guided probe studded with three reflecting balls for motion capture is presented in Figure 2. All three velocity components, static and dynamic pressure are measured with a five-hole pitot probe and interpolated onto a regular grid and presented on a screen in real time. The latency is $4 ms$. This
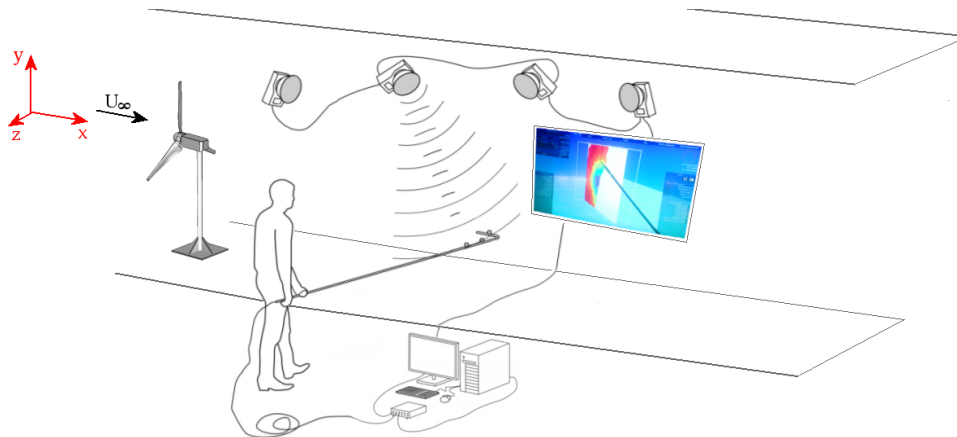
Figure 2. ProCap measurement system installed in the wind tunnel. Four motion capture cameras, a hand-guided probe and real-time projection of the measurement data are set up in the wake area behind the model wind turbine. The wind tunnel side walls (not shown in sketch) are located at $z/R = \pm 6$, while the floor and roof are located at $y/R = \pm 4$.
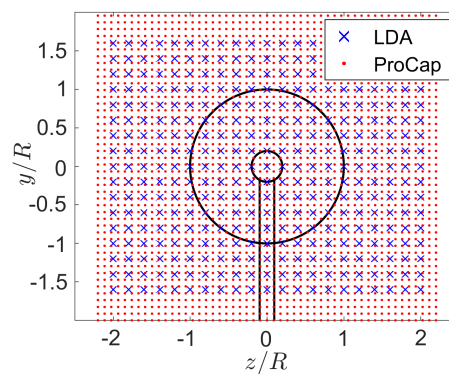

Figure 3. Measurement grids of the LDA (blue) and the ProCap system (red).

allows the operator to adjust the position of the probe and measurement point density according to the actual flow field and thus focus on specific areas. For the presented measurement a spatial resolution of of $2\,cm$ was chosen, resulting in a grid of 2346 measurement points per full wake scan (see Figure 3). The total measurement time for a full wake scan at this resolution is at the order of 10 minutes. The data is tracked in real-time, but also remains available for later post-processing and comparison with other datasets, e.g. in ParaView or Matlab [13].

3.4. Quantification of wake deflection
As observed in earlier measurements, the wake behind a yawed wind turbine is highly asymmetrical and develops a curled shape for higher downstream distances [3]. For this reason a quantification of the wake center is not straightforward. A number of different methods for the wake center detection have been suggested in order to make deflection results comparable. Vollmer et al. [5] discussed several of these methods, amongst them two- and three-dimensional Gaussian fitting methods of the measured or simulated wake profile. Also, a method that calculates the theoretical available power for an imaginary downstream rotor was used, which has been proven to be a suitable method to quantify the deflection of the energy deficit contained in the wake. This method is therefore also used in this study. The procedure is explained in

Table 1. Overview of test cases and measurement techniques applied.

Downstream distance x/D [-]	Yaw angle γ [°]	ProCap data	LDA data	Validation performed
1-15	30	-	line profile	-
3	30	full contour	full contour	yes
6	30	-	full contour	-
9	-30	full contour	-	-
9	0	full contour	line profile	-
9	10	full contour	-	-
9	20	full contour	-	-
9	30	full contour	full contour	yes
12	30	-	full contour	-
15	30	-	full contour	-

detail in a recent paper by Schottler et al. [14].

3.5. Measurement uncertainty

The statistical uncertainty of the individual measurement points of the mean velocity in the LDA measurement is assessed according to the procedure proposed by Wheeler and Ganji [16]. Precision errors are calculated from the standard deviation in the time series based on a 95 % confidence interval. The precision error is then combined with a systematic error based on the calibration of the reference velocity to a total error.

The uncertainty of the ProCap measurements is calculated following the procedure described by Müller [15]. The precision error is computed for the discrete measurement points, taking into account a calibration error and a probe tracking error from a pre-experiment in a well-known reference flow. The total error is then calculated from the precision error combined with a systematic error obtained from the calibration of the wind tunnel reference velocity. Uncertainties due to errors in the interpolation process are omitted for both measurement techniques.

3.6. Test case overview

Various measurements in the wake behind the yawed turbine have been performed, using both the LDA and ProCap system. Three full wake scans at different downstream distances and yaw angles have been performed with both techniques in order to be able to validate the ProCap system against the well-established LDA technique.

Line wake profiles have furthermore been measured all downstream distances from x/D=1-15 using the LDA, while full wake contours have been recorded for x/D=3, 6, 9, 12 and 15. At x/D=9, the turbine's yaw angle is varied from γ= -30°, 0°, 10°, 20° and 30°, while the wake is measured using the ProCap system. All investigated test cases are listed in Table 1.

4. Results

4.1. Validation of ProCap measurement technique

At first the wake results, which have been performed with both measurement techniques are compared. This is done to validate the ProCap measurement system against the LDA technique and prove its applicability for high-resolution wake measurements. From a physical point of view, the two techniques are very different as LDA measures the flow velocity from the frequency shift of a backscattered laser beam, while the ProCap system is a pressure-based flow measurement technique. In total, a comparison of three full area wake measurements is performed. The
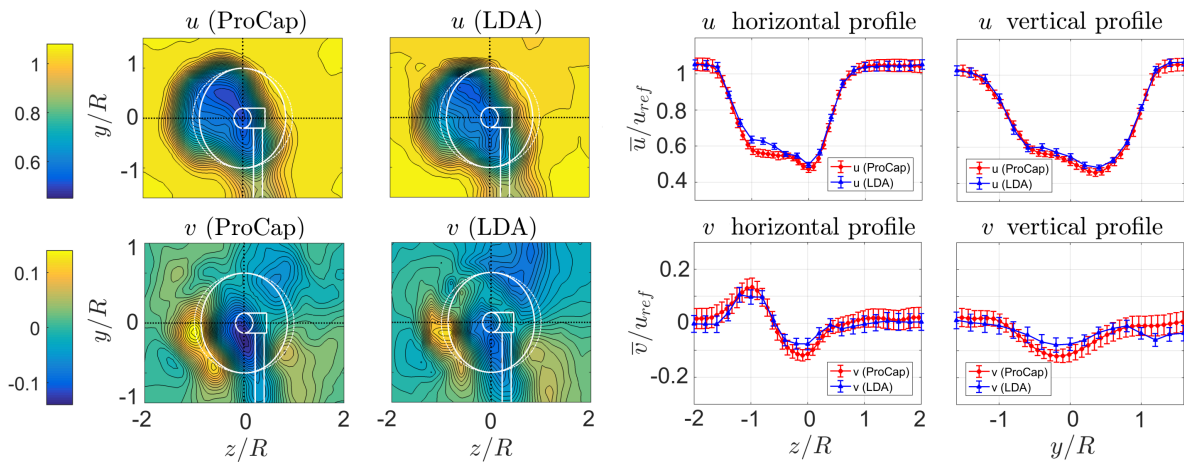
EERA DeepWind'2018, 15th Deep Sea Offshore Wind R&D Conference

IOP Conf. Series: Journal of Physics: Conf. Series **1104** (2018) 012018

IOP Publishing

doi:10.1088/1742-6596/1104/1/012018

Figure 4. Comparison of the mean flow components u and v at $x/D = 3$ and $\gamma = 30°$

first comparison shown in Figure 4 depicts the mean flow components u and v in the wake at $x/D = 3$ for an upstream turbine yaw angle of $\gamma = 30°$. At this downstream distance, the flow still features rather pronounced gradients in both components. The results obtained with the ProCap system show an accurate agreement with the LDA reference experiment. The gradients of streamwise flow component u are well captured by the ProCap system and compared well with the reference LDA results. Also the vertical flow component v is observed to compare well with the reference data measured by the LDA. Areas of strong rotation in the flow are accurately resolved. A direct comparison of the flow profiles at hub height, as shown on the right hand side of Figure 4, only show minor deviations in the wake center. These can be attributed to a coarser measurement grid applied for the LDA measurements and inaccuracies in the measurement setup. A closer look reveals slower free stream velocities outside the wake in the upper half of the LDA contour plots. It is assumed that this is due to an influence of the traversing system on which the LDA probe is mounted on. The traversing system blocks about 10% of the wind tunnel cross sectional area underneath the roof. For the ProCap measurements no traversing system is applied, as the hand-guided probe is moved through the measurement volume from outside the wind tunnel through a small opening. The clockwise rotation of the wake flow at
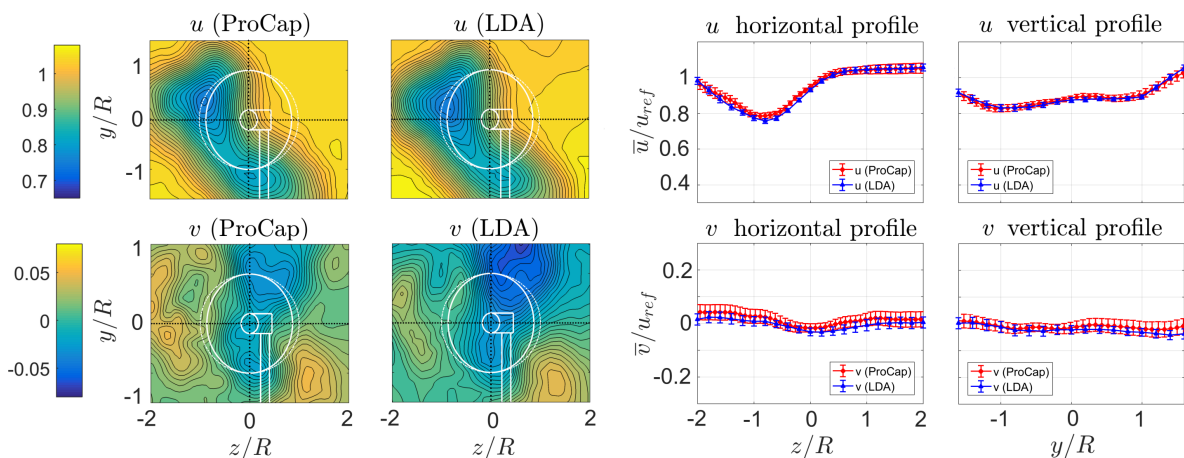

Figure 5. Comparison of the mean flow components u and v at $x/D = 9$ and $\gamma = 30°$

$x/D = 3$ is well observed in the vertical flow component shown in the lower part of Figure 4. The swirl in the wake is well resolved by the ProCap system, although larger maximum or minimum vertical velocities are measured. A strong downward flow underneath the wind tunnel roof is also observed in the v-component, which again can be attributed to a local blockage by the traversing system.

An almost perfect match in the results mean streamwise flow component u is obtained for the wake of a $\gamma = 30°$ yawed turbine at $x/D = 9$ as shown in Figure 5. The flow gradients are significantly weaker at this downstream distance resulting in a excellent agreement between the results obtained by the two measurement techniques. Also, the vertical flow component compares well for this test case, especially in the lower part of the measurement volume.

In conclusion, the ProCap measurement system proved to accurately recreate the results obtained by the LDA measurements for both the streamwise and the vertical flow component. The deviations found in the results between the two techniques can be attributed to imperfections in the LDA setup, especially a blockage influence by the traversing system in the upper half of the measurement volume. In regions of strong flow gradients contour plots derived from ProCap measurements are seen to be smoother, due to a finer resolution of the measurement grid.

4.2. Yaw angle variation

The ProCap system moreover has the benefit that all three flow components u, v and w are measured simultaneously. This feature is taken advantage of for an analysis of the mean wake characteristics at different yaw angles. As presented in Figure 6, the yaw angle is varied from $\gamma = [0°, 10°, 20°, 30°]$. For an assessment of the wake symmetry with respect to the turbine yaw angle an additional wake measurement at $\gamma = -30°$ is performed. The wake's lateral deflection is observed to increase with upstream turbine yaw angle. For yaw angles $\gamma = 20°$ and $30°$, a curled wake shape as previously reported is seen. An analysis of the flow components v and w in the yz-plane discloses a counter-rotating vortex pair wake area at these yaw angles. The vortices create a strong lateral flow in the center of the wake, pushing the wake to the side as indicated by the vector field in Figure 6. The mean wake flow at $\gamma = -30°$ is observed to be very different to that of the turbine yawed in the corresponding positive direction. This asymmetry is deemed to stem from a significant interaction of the wake flow with the turbine tower and nacelle. Compared to measurements on a larger rotor ($D = 0.90\,m$) by Bartl et al. [6], the asymmetry on the smaller rotor is more pronounced due to a larger impact of tower and nacelle.

4.3. Far wake development

In the optimization process of a wind farm layout, wake steering can already have a significant influence in the design phase. For this purpose, accurate predictions of the wake deflection for different downstream distances are important to find the economically most feasible layout. Simple analytical prediction models for the wake deflection have been developed by Jiménez et
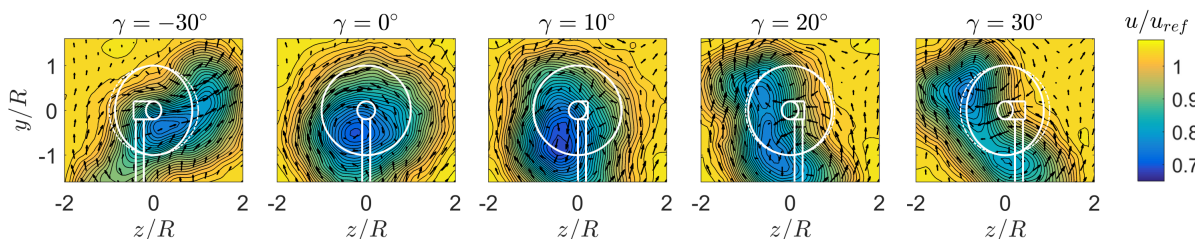

Figure 6. Mean streamwise flow component u/u_{ref} at $x/D = 9$ and $\gamma = -30, 0, 10, 20, 30°$ recorded with ProCap. Vectors indicate normalized flow components v and w in the yz-plane.

al. [9] and Bastankhah and Porte-Agél [4]. These models require a validation by experimental results for turbines of different scales and different turbulent environments. In this study, we therefore analyze the far wake development of yawed wake behind the turbine up to $x/D = 15$ in a low-turbulent environment. Full contour scans of the wake behind a $\gamma = 30°$ yawed turbine for the downstream distances $x/D = 3, 6, 9, 12$ and 15 are presented in Figure 7. The wake contours disclose an increasing lateral wake deflection with increasing downstream distance, while the velocity deficit in the wake simultaneously recovers. From a downstream distance of $x/D = 6$ a curled wake establishes, while the wake is observed to split up into two local velocity minima from about $x/D = 9$. These local velocity minima seem to curl around the area behind the rotor and are observed to be almost completely deflected outside of the rotor swept area for $x/D = 15$. The magnitude of the velocity deficit in the wake is observed to decrease at a similar rate to the wake behind a non-yawed turbine (see Garcia et al. [12]). While local velocity deficits of $u_{ref} - u_{wake}/u_{ref} = 0.55$ are measured at $x/D = 3$, the velocity recovers to $u_{ref} - u_{wake}/u_{ref} < 0.20$ at $x/D = 15$.

The investigated inflow turbulence level of TI=0.23% is unrealistically low compared to realistic atmospheric conditions. Depending on the atmospheric stability, realistic turbulence levels would roughly range between 5 and 15% [5]. As shown in another experiment by Bartl et al. [6], the increased mixing due higher inflow turbulence levels would result in a faster recovery of the velocity deficit in the wake. Although the wake of a turbine exposed to higher background turbulence features smoother velocity gradients and a less pronounced curl, the overall deflection of the wake was observed to be similar than for low inflow turbulence [6]. The widely discussed topic of wake meandering was not observed in this set of wake experiments, as no dominant meandering frequencies were detected in the spectral content of the wake flow. It is assumed that the large relative size of the rotor compared to the length scales in the inflow suppresses a significant meandering of the wake. However, a strongly intermittent flow was found in a ring surrounding the mean velocity deficit by the means of two-point statistics in a study by Schottler et al. [7]. This intermittency can be interpreted as a switching between wake state and freestream state in the boundary regions of the wake.

A top view on the wake trajectory in the xz-plane is presented in Figure 8. The iso-map is interpolated from line wake measurements at the turbine's hub height at every rotor diameter from $x/D = 1 - 15$. For a quantification of the wake center deflection the single wake profiles have been fitted with a Gaussian. The minima of fit curves are plotted as a white line. As the wake flow has a very three-dimensional shape in the yz-plane (Figure 7), wake profiles measured at hub height might not really be representative for the three-dimensional kinetic energy distribution in the wake. For this reason, the available power method as described in Section 3.4 is applied, in order to provide an approximation of the deflection of the minimum kinetic energy. The available power deflection is plotted as red star symbols in Figure 8. The deflection approximated by a 2D Gaussian fit is observed to be smaller than the deflection of the 3D available power in the wake for all downstream distances.
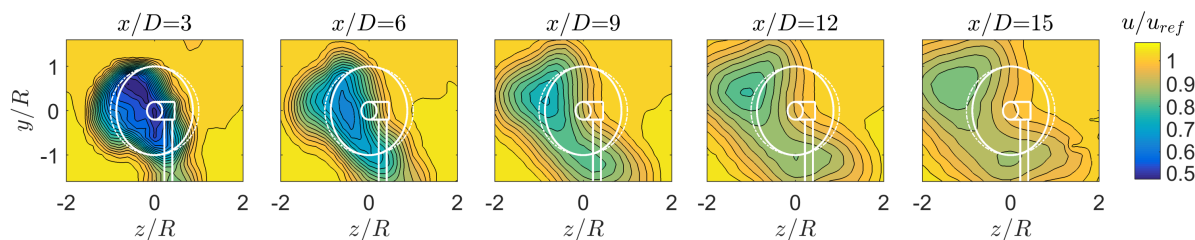

Figure 7. Mean streamwise flow component u/u_{ref} at $x/D = 3, 6, 9, 12, 15$ and $\gamma = 30°$ recorded with LDA.

EERA DeepWind'2018, 15th Deep Sea Offshore Wind R&D Conference

IOP Publishing

IOP Conf. Series: Journal of Physics: Conf. Series **1104** (2018) 012018
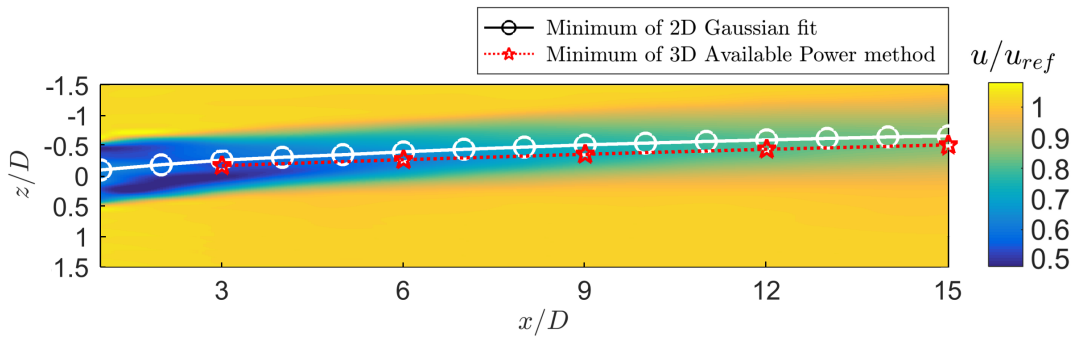
doi:10.1088/1742-6596/1104/1/012018

Figure 8. Top view on the wake trajectory behind a turbine yawed $\gamma = 30°$. Mean streamwise flow component u/u_{ref} in the xz-plane measured at hub height $y/D=0$ ($y_{hub}=0.90\,m$). The white line approximates of the wake center deflection by a 2D Gaussian fit of the measured wake profiles. The red line indicates the deflection of the available kinetic power in the wake.

4.4. Prediction of wake deflection
Finally, the wake deflection measured for different downstream distances in the model experiment is compared to deflection predictions by the engineering models by Jiménez et al. (JCM) [9] and Bastankhah and Porte-Agél (BPA) [4]. The recommended model-parameters as suggested in [9] and [4] were applied for both wake deflection models. In the case of the JCM-model, a linear wake expansion factor of $\beta = 0.125$ was implemented, while $k_y = 0.022$, $k_z = 0.022$, $\alpha^* = 2.32$ and $\beta^* = 0.154$ were used as parameters for the BPA-model. Both models require the thrust coefficient as an input parameter, which was set to the measured value of $C_{T,30°} = 0.63$ in both cases. The BPA-model moreover allows for a modification of the background turbulence intensity as an input parameter, which was set to $TI = 0.23\%$ as measured in the empty wind tunnel environment. The measured and predicted results are compared in Figure 9. Taking the Gaussian fit approximation of the measured results as a reference, the JCM model is observed to constantly overpredict the wake deflection for all downstream distances. The BPA-model, however, is seen to predict the wake deflection sufficiently well up $x/D = 6$. For higher downstream distances also the BPA-model is observed to overestimate the lateral wake deflection significantly. For higher background turbulence levels, the wake deflection predicted
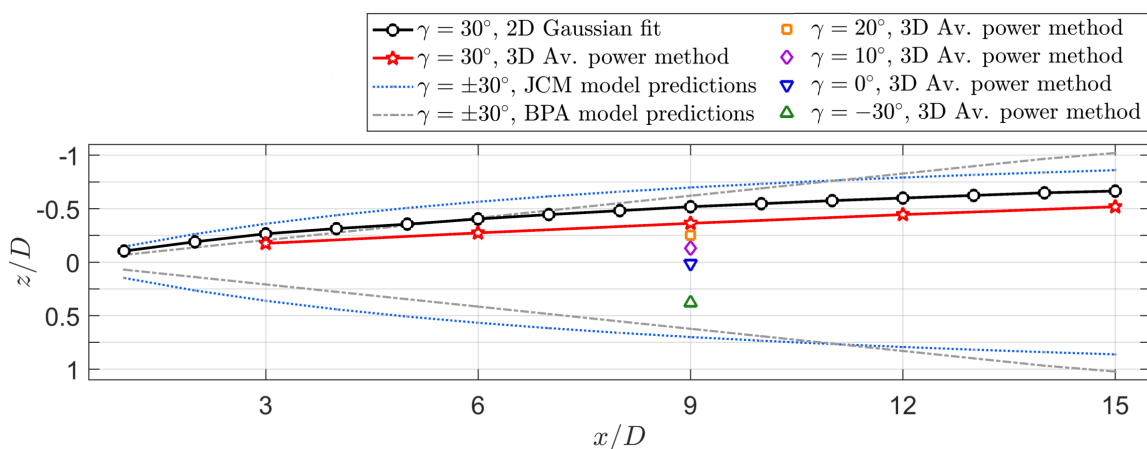

Figure 9. Calculated wake deflection $\delta(z/D)$ behind the rotor ($D = 0.45m$) compared to predictions by deflection models by Jiménez et al. [9] and Bastankhah and Porte-Agél [4].

by the BPA-model has a more asymptotic behavior as shown in a wake-deflection-comparison for different turbulence intensities by Bartl et al. [6]. As suggested by Bastankhah and Porte-Agél [4], the model's sensitivity to inflow turbulence has to be further tested and modeling parameters α^* and β^* adjusted.

5. Conclusions

The capability of the real-time measurement system ProCap for full field flow measurements in the wake of a model-scale wind turbine was demonstrated. Flow results have been compared to results obtained by the well-established LDA technique, validating the ProCap technique in three designated test cases. The ProCap system has proven to detect strong gradients in the flow at the time of the measurement, offering the possibility to focus on such regions and locally refine the measurement grid in these areas. This significantly reduced the measurement time and with that represented the biggest advantage of the manually guided ProCap measurement system over a fully automated traversing system. While a full two-dimensional wake measurement of 350 points takes about 5 hours with a conventional traversing system, the measurement time for a comparable spatial resolution can be reduced to about 10 minutes with ProCap. This corresponds to a speed-up by a factor of 30 in terms of measurement time. Beyond that, the ProCap system features a comparatively simple experimental setup, which opposed to LDA or PIV techniques requires no seeding. Moreover, the real-time data acquisition and processing enables the operator to discuss the results while the measurements are taking place. The full potential of the method for wind turbine wakes will have to be investigated in further measurements. While LDA remains to have its authority for high-fidelity and time-resolved measurements, ProCap appears to greatly facilitate and speed up larger wake surveys and will thus enhance the understanding of the complex flow topology in wind turbine wakes.

References

[1] Gebraad P M O, Teeuwisse F W, van Wingerden J W, Fleming P A, Ruben S D, Marden J R and Pao L Y 2016. *Wind Energy* **19** 95–114 ISSN 1099-1824
[2] Krogstad P Å and Adaramola M S 2012. *Wind Energy* **15** 743–756 ISSN 1099-1824
[3] Howland M F, Bossuyt J, Martínez-Tossas L A, Meyers J and Meneveau C 2016 *Journal of Renewable and Sustainable Energy* **8** 043301
[4] Bastankhah M and Porté-Agel F 2016. *Journal of Fluid Mechanics* **806** 506–541 ISSN 0022-1120
[5] Vollmer L, Steinfeld G, Heinemann D and Kühn M 2016. *Wind Energy Science* **1** 129–141 ISSN 2366-7451
[6] Bartl J, Mühle F, Schottler J, Sætran L, Peinke J, Adaramola M and Hölling M 2017. In review *Wind Energy Science Discussions* URL https://doi.org/10.5194/wes-2017-59
[7] Schottler J, Bartl J, Mühle F, Sætran L, Peinke J and Hölling M 2017. In review *Wind Energy Science Discussions* URL https://doi.org/10.5194/wes-2017-58
[8] Mühle F, Schottler J, Bartl J, Futrzynski R, Evans S, Bernini L, Schito P, Usera G, Draper M, Kleusberg E, Henningson D, Hölling M, Peinke J, Adaramola M and Sætran L 2018. In review *Wind Energy Science Discussions* URL https://doi.org/10.5194/wes-2018-30
[9] Jiménez A, Crespo A and Migoya E 2010. *Wind Energy* **13** 559–572 ISSN 1099-1824
[10] Sarmast S and Mikkelsen R F 2013. The experimental results of the nrel s826 airfoil at low reynolds numbers. *Technical Report DTU*
[11] Chamorro L, Arndt, R and Sotiropoulos F 2012. *Wind Energy* **13** 733–742 ISSN 1099-1824
[12] Garcia L, Vatn M, Mühle F and Sætran L 2017. *Journal of Physics: Conference Series* **854** 012015
[13] Streamwise.ch 2016. Procap system - a standalone system for windtunnel measurements, *Flyer* URL http://www.streamwise.ch/wp-content/uploads/2016/12/2016_07_flyerProCap_system.pdf
[14] Schottler J, Mühle F, Bartl J, Peinke J, Adaramola M S, Sætran L and Hölling M 2017. *Journal of Physics: Conference Series* **854** 012032
[15] Müller A 2017. Real-Time 3D Flow Visualization Technique with Large Scale Capability. *PhD thesis, ETH Zurich* URL https://www.research-collection.ethz.ch/handle/20.500.11850/228428
[16] Wheeler A and Ganji A 2010. Introduction to Engineering Experimentation. *Pearson Education, Upper Saddle River, New Jersey, USA, third edition edn.*